Journal of the Meteorological Society of Japan, Vol.79, No.1B, pp.575–588, 2001

Impact of the Preceding El Niño on the East Asian Summer Atmosphere Circulation

By **Yafei Wang**

Chinese Academy of Meteorological Sciences, Beijing, China

Bin Wang

International Pacific Research Center and Department of Meteorology, School of Ocean and Earth Science and Technology, University of Hawaii, USA

and

Jai-Ho Oh

Meteorological Research Institute, Korea

(Manuscript received 5 January 2000, in revised form 3 October 2000)

Abstract

This paper examines the relationship between the East Asian summer monsoon and the El Niño Southern Oscillation (ENSO) during the period from 1958 to 1998, which is quite different from the link between the South Asian summer monsoon and ENSO.

Major findings are: (1) A new index, called the East Asian Monsoon Index (EAMI), is defined for measuring the East Asian monsoon, which could extensively describe the south-north distribution of the East Asian summer monsoon's activity. The interannual variability of the EAMI displays a significant negative correlation with the broad-scale Asian monsoon index proposed by Webster and Yang (1992) from 1976 to 1998. (2) A significant positive correlation between the summer 500 hPa geopotential height anomalies and the NINO-3 SST in the preceding fall and winter is found in the subtropical regions of East Asia and the western North Pacific, and in northeast Asia centered at 70°N, 137.5°E. A strong (weak) summer monsoon in the subtropical regions of East Asia tends to occur about two to three seasons after the NINO-3 SST anomalies exceed 1.5 ℃ (drop below −0.7 ℃). (3) The above results suggest a delayed impact of the ENSO on the East Asian summer atmosphere circulation. During the summer after the El Niño reaches its mature phase, an anomalous blocking anticyclone tends to occur in northeast Asia. Meanwhile a subtropical high of the western North Pacific extends abnormally westward. This anomalous circulation pattern enhances the summer monsoon in subtropical East Asia. The abovementioned evolution of the circulation anomalies became more prominent in the unprecedented '97/98 El Niño event, suggesting that the devastating 1998 flood in southern central China may be partially due to the delayed impact of the '97/98 El Niño.

The physical processes for the delayed impact besides the air-sea interaction in the tropical and subtropical western Pacific are discussed too.

Corresponding author: Yafei Wang, Chinese Academy of Meteorological Sciences, Baishiqiao road 46, Haidian, Beijing, 100081, China.
E-mail: yfwang@public.east.cn.net

1. Introduction

A new era in climate dynamics has evolved since Bjerknes (1966 and 1969) first established the physical linkage between the Southern Oscillation (Walker and Bliss 1932) and the Pacific basin-wide warming (El Niño). The influence of ENSO on the Asian Monsoon has been extensively examined in the last two decades. Mooley and Parthasarathy (1983) found that deficient Indian summer monsoon rainfall tends to occur in the year when an El Niño event develops. Webster and Yang (1992) defined a broad-scale circulation index to measure the intensity of the Asian monsoon. They pointed out that a weak Asian summer monsoon is often associated with the development of an El Niño event. With an understood atmospheric general circulation model, Yang and Lau (1998) found that the forcing from the positive SST anomalies over the east central Pacific in an El Niño year reduces land-sea thermal contrast over the Asian continent, resulting in a weak Asian summer monsoon. Based on the above results, Kawamura (1998) suggested a possible mechanism for Asian summer monsoon-ENSO interaction, which links the evolution of the large-scale circulation with the continental land surface processes and the feedback of anomalous SST in the eastern Pacific. In general, most studies have been focused on the impacts of ENSO on the South Asian summer monsoon.

Zhang et al. (1996) found that the East Asian summer monsoon intensified during the mature phase of the '86/87 El Niño. This indicates that the behavior of the East Asian summer monsoon appears to be somewhat different from that of the South Asian summer monsoon. Zhang et al. (1996) argued that during the climax of El Niño, the convective activity around the equatorial western Pacific is strongly suppressed, which exerts significant influences on the East Asia climate. They emphasized the concurrent relationship between the height of ENSO warming and the East Asian monsoon. However, the '86/87 event is exceptional as it matured in the summer of 1987, whereas the ENSO warm events normally mature in the boreal winter (Rasmusson and Carpenter 1982).

As shown in Fig. 1, the summer precipitation in China varies significantly in the year during which the ENSO decays (reference is page 223–225 of Ye and Huang 1996). There are two anomalous rainfall belts, one in southern central China (the south of Changjiang River) and the other stretching from northwest to northeast China. This statistical result has not received a full physical explanation. Recently, Wang et al. (2000) reveal that during the mature and decay phases of major ENSO events, an anomalous low-level anticyclone occurs over the Philippine Sea due to cooling of the sea basin. The anticyclone develops rapidly in late fall of the year when a strong warm event matures. This anticyclone persists until the following spring or early summer, causing anomalous wet/dry conditions along the East Asian front stretching from south central China northeastward to east of Japan (Kuroshio extension). The development of the anticyclone is nearly concurrent with the enhancement of in situ sea surface cooling. The mechanism responsible for the development and persistence of the western North Pacific subtropical anticyclone is a positive thermodynamic feedback between the anticyclone anomaly and the sea surface cooling in the presence of mean northeasterly trades during the boreal cold season (Wang et al. 2000). Their analysis and theory are confined to the subtropics and tropics.

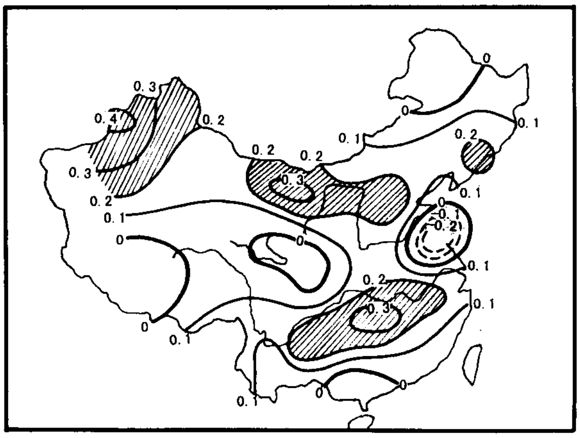

Fig. 1. Composite map of precipitation percentage anomalies in summer during the next years of the onset of El Niño episodes from 1950 to 1993 (adopted from Ye and Huang, 1996). Shaded areas show the value over 0.2 (20%).

A number of previous studies have pointed out that the East Asian monsoon is different from the Indian monsoon in its structure and evolution (Tao and Chen 1987; Ding 1994). The East Asian monsoon is generally referred to as the area bounded by 20°N and 40°N latitudes and 110°E and 140°E longitudes (Zhang et al. 1996). The South Asian monsoon is a tropical phenomenon that is characterized by the annual reversal of the low-level zonal wind component, whereas the East Asian monsoon is a subtropical/midlatitude entity characterized by the annual reversal of the meridional wind component. The reversal of meridional wind in the East Asian Summer monsoon can be attributed to the east-west thermal contrasts between the Asian continent and the Pacific Ocean. Also quite different features from the tropical monsoon are the influence of a mid-latitude frontal system, called Meiyu/Baiu front. On the other hand, the annual reversal of zonal winds in South Asia should result from the north-south thermal contrast between the Indian Ocean and the Asian land mass (it is also enhanced by the effects of the Tibetan Plateau). Ninomiya and Kobayashi (1998) defined major circulation systems that related with the variations of the Indian rainfall and East Asian rainfall (especially Meiyu/Baiu rainfall), respectively. The onset, withdrawal, and peak of the rainy season exhibit remarkable differences in the East Asian and South Asian monsoon regions. The South Asian tropical monsoon is characterized by steep annual range of rainfall, long duration (over four months in general), and equatorward retreat of rain-belt. The East Asian subtropical-midlatitude monsoon, on the other hand, shows rather different features. A prominent discontinuity on the map of peak rainfall time, defined by a line extending from Hainan island (21°N, 110°E) to the region of 25°N, 145°E, has divided the East Asian and western North Pacific monsoons. Evidently these two regions are highly influenced by the movement of the western Pacific Subtropical high.

Four questions concerning the relationship between ENSO events and the East Asian summer monsoon remain to be answered: (1) What are the relationships between the East Asian summer monsoon and the South Asian summer monsoon in their interannual variability? (2) How to define an adequate index for describing such an East Asian summer monsoon? (3) How do ENSO events exert a delayed impact on the East Asian summer monsoon? (4) What physical processes are responsible for the delayed impact besides the air-sea interaction in the tropical and subtropical western Pacific?

The aim of this paper is to address the first three questions by examining observations. The fourth question will also be discussed in the last section.

2. Data and analysis procedure

The NCEP/NCAR (National Centers for Environmental Prediction/National Center for Atmospheric Research) global atmospheric reanalysis dataset, covering a 41-year period from January 1958 to December 1998, was the primary dataset used for this study. A detailed description of the data assimilation system that produces this dataset is given by Kalnay et al. (1996). The data assimilation system was based on the global forecast model that was implemented operationally at NCEP in January 1995. The observational database includes considerable amounts of data that were not available in real time. A spectral statistical interpretation and a three-dimensional variational analysis method were adapted for the data assimilation. We used monthly mean data on standard pressure surfaces gridded onto a 2.5° latitude/longitude grid. In addition, we used monthly SST data from NINO-3 area compiled by Climate Prediction Center/NCEP from 1957 to 1998. NCEP optimum interpolation (OI) analysis of SST (Reynolds and Smith 1994) gridded onto a 2° latitude/longitude grid is also used. Monthly rainfall data from 160 Chinese meteorological stations (1958 to 1998) used in this study were obtained from the National Climate Center of China.

3. Relationships between the East Asian and South Asian summer monsoon

Although the differences between the East Asian and South Asian monsoons have been well recognized, the difference and linkage between the variability of the East Asian and South Asian summer monsoons has not been well documented and understood.

To measure the interannual variation of the South Asian summer monsoon, Webster and Yang (1992) defined a "broad-scale circulation" index (WYI hereafter) based on the consideration of the relationship between the thermal wind and meridional temperature gradient that exists between the Asian continent and the Indian Ocean. This index is defined by the vertical zonal wind shears between 850 and 200 hPa averaged over the region (0–20°N, 40–110°E). The WYI represents the variability of the active center of the westerly shears of the Asian monsoon, and the convective variability in the entire region of South Asia; it includes the convection centers located in the Bay of Bengal and the vicinity of the Philippines (Wang and Fan 1999). The WYI as a whole is a very adequate measure of the strength of the broad-scale South Asian tropical monsoon.

The definition of a meaningful monsoon index for the East Asian summer monsoon is an issue and concern of current research (Wang and Fan 1999, and Lau et al. 2000). In this paper, we propose a new East Asian monsoon index which is defined by the difference between the summer

(JJA) mean 850 hPa southerly anomalies averaged over the area EA II (the southern portion of the monsoon domain 20–30°N, 110–140°E) and over the area EA I (the northern part: 30–40°N, 110–140°E). The onset, peak, and withdrawal of the East Asian monsoon rains start from about 22°N and progress northward, accompanying the northward march of the western Pacific subtropical high. The southerly moisture transport from the three major circulation systems in situ plays an important role in keeping the Meiyu/Baiu front active (Ninomiya and Kobayashi 1999). The position of the subtropical high and monsoon rain belt (including the Meiyu/Baiu frontal zone) vary significantly from year to year (Wang 1993). Therefore, it is very important to know where the East Asian summer monsoon would be most active for the purpose of seasonal prediction (National Climate Center 1998).

The EAMI reflects the prevailing position (south or north) of the East Asian summer monsoon systems. A large value of EAMI means strong summer monsoon staying mainly in the southern part of East Asia (the EA II area) and vice versa. This can be seen from Figs. 2a and 2b which show the composite anomaly maps of the 850 hPa winds and geopotential height for the years of large positive (0.21 ms^{-1}) and negative (-0.42 ms^{-1}) EAMI, respectively[1]. During high EAMI years, southwesterly anomalies dominate the EA II area (Fig. 2a), indicating stronger than normal summer monsoons. Weaker southwesterly wind anomalies exist in the EA I area. In contrast, for the low EAMI composite, there exist northeasterly wind anomalies in the EA II area, indicating weak summer monsoons (Fig. 2b). In the EA I area, weak southwesterly and anticyclonic circulation occur, suggesting a dipole vorticity pattern.

Note also that during high EAMI years, positive Z850 anomalies are located around the Cherski Mountains (to the northwest of the Okhotsk Sea) and the EA II area, while the negative anomalies occur to the east of Hokkaido Japan (Fig. 2a). The anomaly centers of Z850 in Fig. 2b are distributed almost oppositely to those in Fig. 2a. The positive center is around Japan and the negative one is around 22.5°N, 130°E. From this it can be seen that the subtropical high (1520 contour line) extends much further westward in the high EAMI

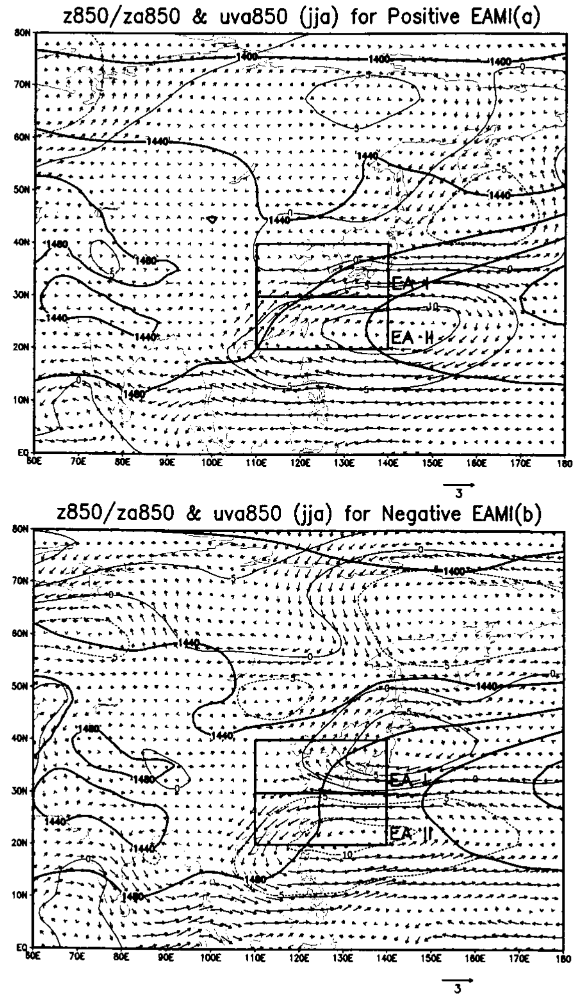

Fig. 2. Composite maps of the 850 hPa winds anomaly (vector, ms^{-1}), geopotential height (thick line, contour interval: 40 gpm) and the height anomaly (thin line, contour interval: 5 gpm) for the years of large positive EAMI (a: 1976, 1977,1979, 1980, 1983, 1987, 1988, 1991, 1993, 1994, 1995, 1996 and 1998) and negative EAMI (b: 1978, 1981, 1982, 1984, 1985, 1986, 1989, 1990, 1992 and 1997). The data used is from 1976–1998. Box area shows the East Asian key region (up pane: EA I area, below pane: EA II area).

years than that in the low EAMI years, which is associated with the Z850 anomalies distribution.

Figure 3 shows the correlation between EAMI and summer rainfall in China from 1976 to 1998. A large significant positive correlation area is notable to the south of 30°N, especially distributed in the regions bounded by 24–30°N, 107–119°E, in-

1 We adopt 23 years' data (summer of 1976–1998) to calculate EAMI (see detailed explanation in the discussions of the Section 6).

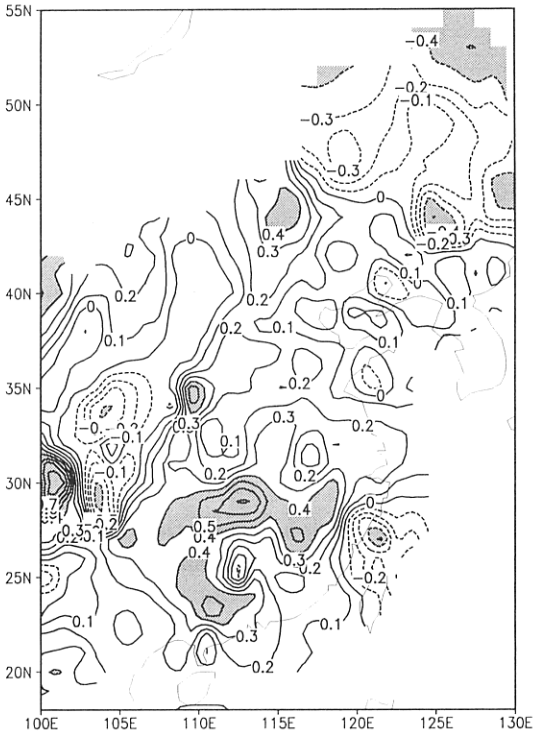

Fig. 3. Seasonal (JJA) correlation map between EAMI and Rainfall in China for the period of 1976–1998. Shaded areas show absolute values over 0.4 (exceeding 95% confidence level).

dicating that the large positive (negative) EAMI supports (abandons) the persistent rain belt (including the Meiyu/Baiu rain belt) staying in the EA II area. Note that the location of the positive correlation corresponds on the southern rainfall belt in Fig. 1. The strong southwesterlies play a role in transporting warm/wet air flow into the EA II area from the ocean (Ding 1994, Ninomiya and Kobayashi 1999), while the weak cold air associated with a blocking high around the Okhotsk Sea invades the Changjiang basin (Wang 1992). These two factors result in keeping the anomalous rain belt to the south of the Changjiang basin. A significant negative region exists around 33°N, 104°E, suggesting an opposite situation upstream of the EA I and II regions.

To investigate the East Asian monsoon relating with the Z500 pattern, the correlation between the EAMI and Z500 in summer is calculated as shown in Fig. 4. A significant positive correlation is centered around 20°N, 145°E (covering most of the areas in the low latitudes) and 65°N, 140°E (around the Cherski Mountains), and a significant negative center is around 40°N, 145°E (to the east of Japan). This implies positive (negative) EAMI associated closely with the anticyclonic (cyclonic) anomalous circulation around the Cherski Mountains and tropical region (to the east of the Philippine Islands), and cyclonic (anticyclonic) anomalies around Japan. Negative and positive centers located at middle and low latitudes are clearly divided by the 30°N line suggesting that EAMI relates with the height field at 500 hPa not limited in the EA I and EA II areas, but in the rather extensive region outside of the two key areas of East Asia. In brief, EAMI representing the East Asian monsoon in EA I and II areas is broadly associated with the middle troposphere atmosphere circulation centered around 140∼145°E in high, middle and low latitudes respectively.

Figure 5 depicts the temporal JJA evolution of EAMI and the WYI from 1976 to 1998. A negative correlation coefficient of −0.41 is found between EAMI and WYI in the last 23 years; this correlation is statistically significant at the 95% confidence level. The negative correlation implies that when the South Asian summer monsoon is strong (weak), the East Asian monsoon is often weak (strong) in subtropical East Asia (EA II area). Note that when the WYI is a minimum (maximum), the EAMI tends to reach maximum (minimum) in the same year or the year after. Since weak South Asian summer monsoon (low WYI) is often associated with El Niño, it is meaningful to examine how the East Asian summer monsoon relates to ENSO events.

4. Relationship between the East Asian summer circulation and ENSO events

4.1 Seasonal correlation

Webster and Yang (1992) showed that the atmosphere circulation in South Asia is poorly correlated with the preceding Southern Oscillation Index (SOI). To see whether this conclusion applies to the East Asian summer monsoon, we examine the seasonal correlation maps between 500 hPa geopotential height (Z500), in summer and the SST anomalies in the NINO-3 area (SST3), from the preceding autumn (SON) to the concurrent summer.

Quite similar correlation patterns are seen distributed in Figs. 6a and 6b. A positive correlation center exceeding 95% significant level between Z500 in JJA and the SST3 from preceding SON to

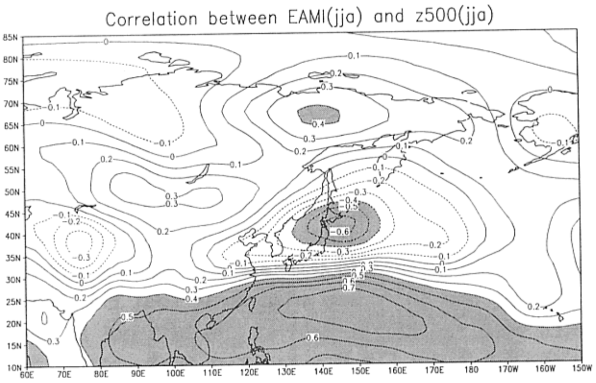

Fig. 4. Seasonal (JJA) correlation maps between EAMI and 500 hPa geopotential height for the period 1976–1998. Shaded areas show absolute values over 0.40 (exceeding 95% confidence level).

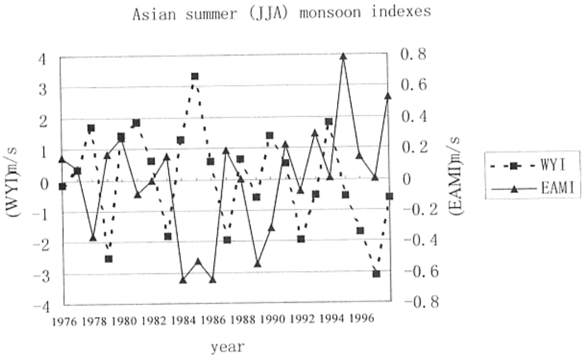

Fig. 5. Time series of the EAMI and WYI in summer (ms^{-1}).

DJF is located around the Cherski Mountains. Another large significant positive correlation area covers the lower latitude, which is centered at 25°N, 180°E with a peak amplitude (over 0.6) stretching into the EA II area. Note that this area is where the subtropical high prevails in the summer season. The positive correlation areas in Figs. 6a and 6b are close to the locations of those in Fig. 4. In fact, EAMI also has a significant correlation (0.487, at 98% confidence level) with the SSTA in the NINO–3 area (SSTA3) in the preceding SON. The significant positive areas in Figs. 6a and 6b mean that the positive (negative) height anomaly will occur in situ two to three seasons after the warm (cold) episode of ENSO. Wang (1992) pointed out that blocking anticyclones around East Asia of higher latitudes (from Lake Baikal to the Okhotsk Sea) occur frequently in summer. He also pointed out that when the stationary wave activity fluxes associated with the blocking high around the Okhotsk Sea propagates from East Siberia via Japan to the subtropics. In association, the eastern part of the Meiyu/Baiu rain belt often shifts southward. In addition, Wang (1992) and Wang and Song (1998) showed that the blocking high around East Asia has a significant positive correlation with Meiyu in China for the formation of a blocking situation is favorable for cold air flowing southward into the Meiyu frontal zone. The significant positive correlation center located around the Cherski Mountains in Fig. 6a basically matches the location of the negative correlation center near the Okhotsk Sea in Fig. 9 of Wang (1992). Although the area of the positive correlation around the Cherski Mountains is much smaller than that around low latitudes, there is no doubt about its robustness. Lag correlations between Z500 and some other ENSO indices (i.e., SOI etc.) show similar results. This finding suggests that the positive height anomaly around the Cherski Mountains associated with the preceding El Niño episode may be contributed to the in situ development of the blocking anticyclone. Likewise, the positive height anomaly covered with the lower latitudes in the preceding warm episodes implies development of a subtropical high in those regions. Note that the most part of the significant positive area in the lower latitudes is located to the south of 30°N, while the mean major subtropical high in summer extends much further to the northeast of the area (National Climate Center 1998). This indicates that the contribution to the subtropical high is limited to a more southwestern area (i.e., closer to the equator).

When approaching summer, the positive correlation areas both in high and low latitude decreases, but the negative area to the east of Japan slightly enhances as shown in Fig. 6c. The significant negative correlation area centered at 42.5°N, 150°E (below −0.4) becomes more evident in Fig. 6d. On the contrary, the positive area around low latitudes shrinks. In order to focus on the impact of the preceding ENSO event on the East Asian summer monsoon, we defer discussion of the negative correlation areas in Figs. 6c and 6d to Section 6.

4.2 Composite characteristics

Since the correlation pattern in Fig. 6a is more significant than that found in Fig. 6b, the SSTA3 (Fig. 7) in autumn (SON) is chosen as a criterion to estimate the impact of ENSO. Figures 8a–d (Figs.

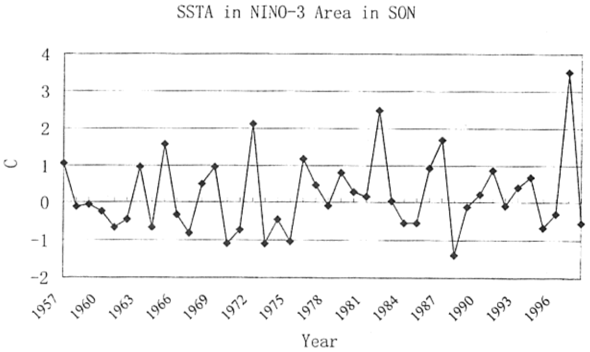

Fig. 7. Evolution of NINO-3 SSTA (℃) in fall season (SON) for the period 1957–1998.

8e–h) show the composite maps of the SSTA distribution from SON to the following JJA for the years when SSTA3 is over 1.5 ℃ (below −0.7 ℃) in the SON. Five samples of warm episodes (1965, 1972, 1982, 1987 and 1997) and six of cold ones (1967, 1970, 1971, 1973, 1975, and 1988) were selected for composition. Note that the warm events contain the most robust El Niño cases in recent decades, such as 1982 and 1997 (see Fig. 7). The distinct warm (cold) SSTA areas are distributed around the central east Pacific in Figs. 8a and 8b (Figs. 8e and 8f), which identifies typical El Niño and La Nina phenomenon occurring in the preceding SON and DJF. And the most obvious ones are in the Fig. 8a and Fig. 8e. The El Niño and La Nina episodes decay and reverse from MAM to JJA. The intensity of the El Niño phenomenon in Fig. 8a is stronger than that of the La Nina phenomenon in Fig. 8e. This is because the absolute value of the composite negative SSTA3 is smaller (about 0.8 ℃) than that of the composite positive SSTA3 (see Fig. 7). Also notice that a quite large opposite SSTA area around the northwestern Pacific frequently exists to that around the central east Pacific in Figs. 8a–h, whose function will be discussed in the Section 6.

Figure 9 illustrates the composite 500 hPa height and its anomalies (Z500A) in the summers selected

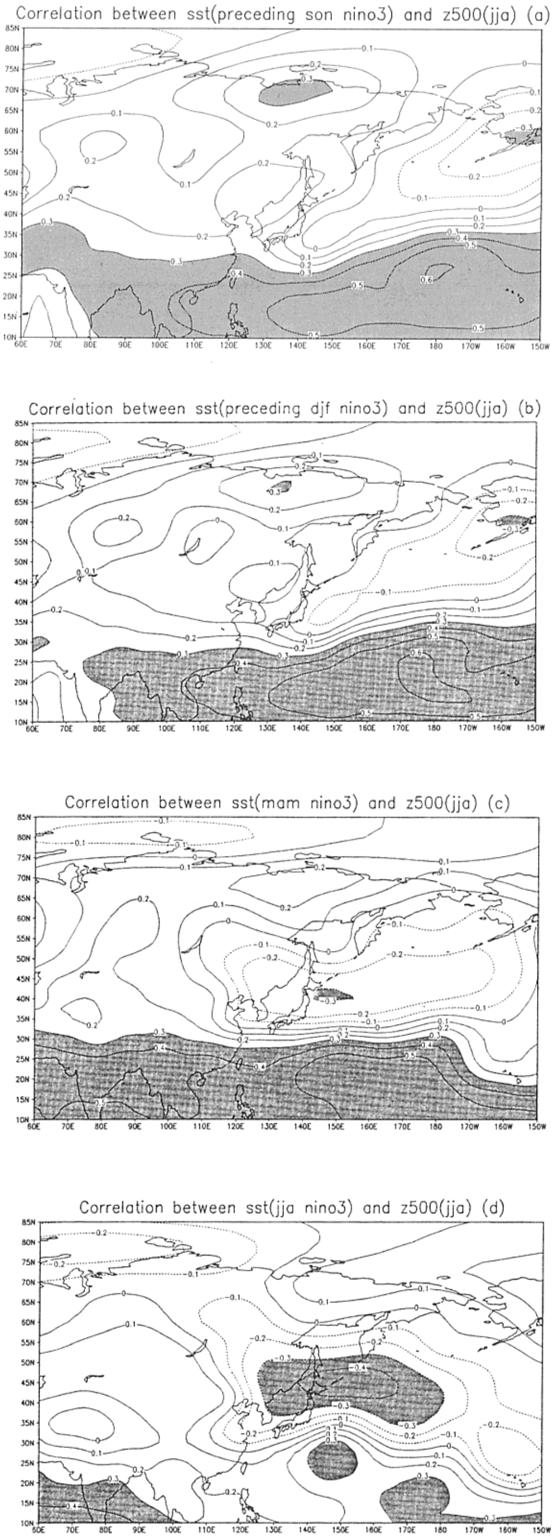

Fig. 6. Seasonal correlation maps between summer (JJA) 500 hPa geopotential height and NINO-3 SSTA in the preceding fall (SON, −1) (a), winter (DJF, −1), spring (MAM, 0) (c), and summer (JJA, 0) for the period of 1957–1998. Shaded areas show absolute values over 0.3 (exceeding 95% confidence level).

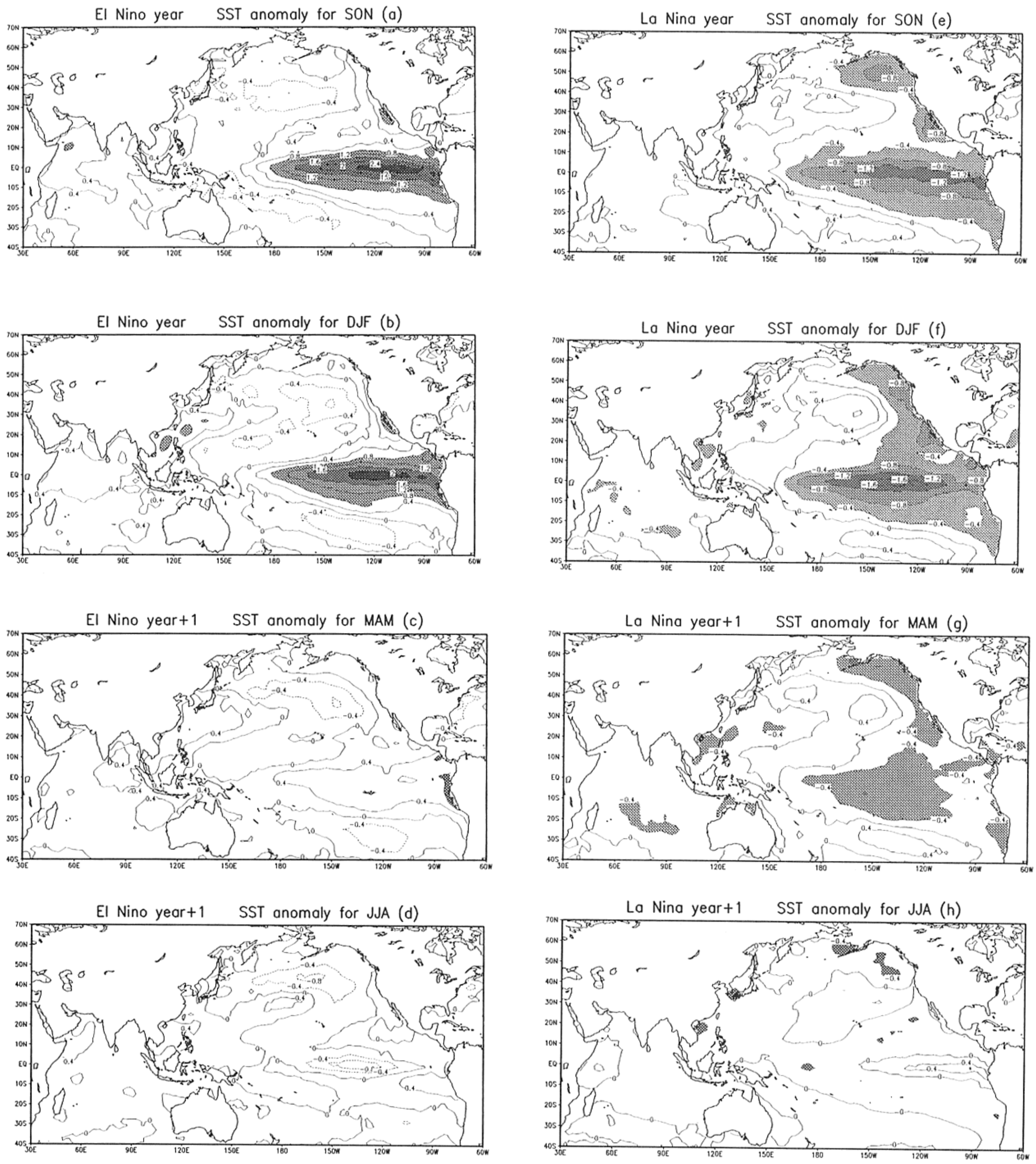

Fig. 8. Composite seasonal SST anomalies for the SON (a), DJF (b), MAM (c) and JJA (d) for El Niño years (1965, 1972, 1982, 1987, and 1997; shaded areas: over 0.8 ℃), SON (e), DJF (f), MAM (g) and JJA (h) for La Nina years (1967, 1970, 1971, 1973, 1975 and 1988; shaded areas: below −0.4 ℃).

by SSTA3 exceeding over 1.5 ℃ (a) and dropping below −0.7 ℃ (b) in the preceding autumns. A strong positive anomaly center (over +25 gpm) is found around the Cherski Mountains (involving the Okhotsk Sea) in Fig. 9a, which is associated with a strong ridge in situ. This positive center is very close to the location of the positive correlation center in Fig. 4 and Figs. 6a and 6b. But compared with the significant area around the Cherski Mountains in Fig. 6a, the strongly positive height anoma-

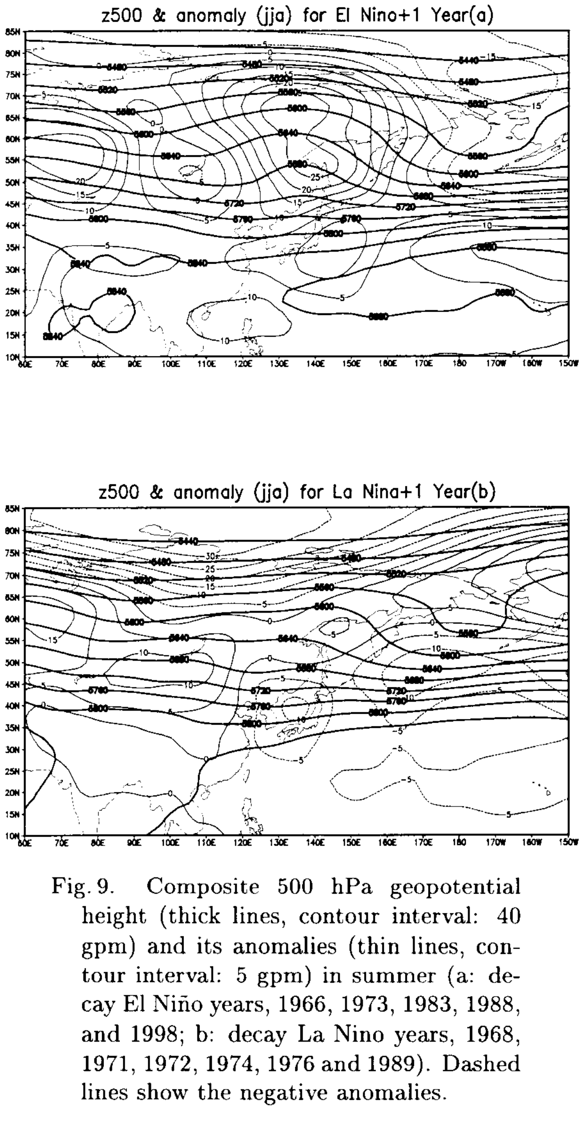

Fig. 9. Composite 500 hPa geopotential height (thick lines, contour interval: 40 gpm) and its anomalies (thin lines, contour interval: 5 gpm) in summer (a: decay El Niño years, 1966, 1973, 1983, 1988, and 1998; b: decay La Nino years, 1968, 1971, 1972, 1974, 1976 and 1989). Dashed lines show the negative anomalies.

lies occupy a much larger area around East Siberia as shown in Fig. 9a. This distinct phenomenon may imply that the preceding El Niño is widely associated with strong ridge or anticyclone around high latitudes of the East Asian region. There is a relatively low height area to the east of Japan, corresponding to the negative correlation center in Fig. 4. The subtropical high, represented by the 5880 gpm contour line, extends westward to 20°N, 130°E; southwest of this high (including the Philippine Islands) is a positive anomaly area (over 10 gpm). This is consistent with the significant positive anomaly around low latitudes in Figs. 6a and 6b.

Figure 10 is the same as Fig. 9 except for the composite geopotential height, geopotential anomaly and wind anomaly at 850 hPa. A significant southwesterly wind anomaly with 0.51 ms^{-1} of EAMI prevailed around the EA II area in Fig. 10a. This southwesterly wind anomaly could transport moisture air into EA II area as a result of favorable summer monsoon rainfall condition in situ. Corresponding to the location of the positive center in Fig. 9a, large positive height anomaly centers (over +15 gpm and +10 gpm) with a ridge are located around the Okhotsk Sea and the Cherski Moun-

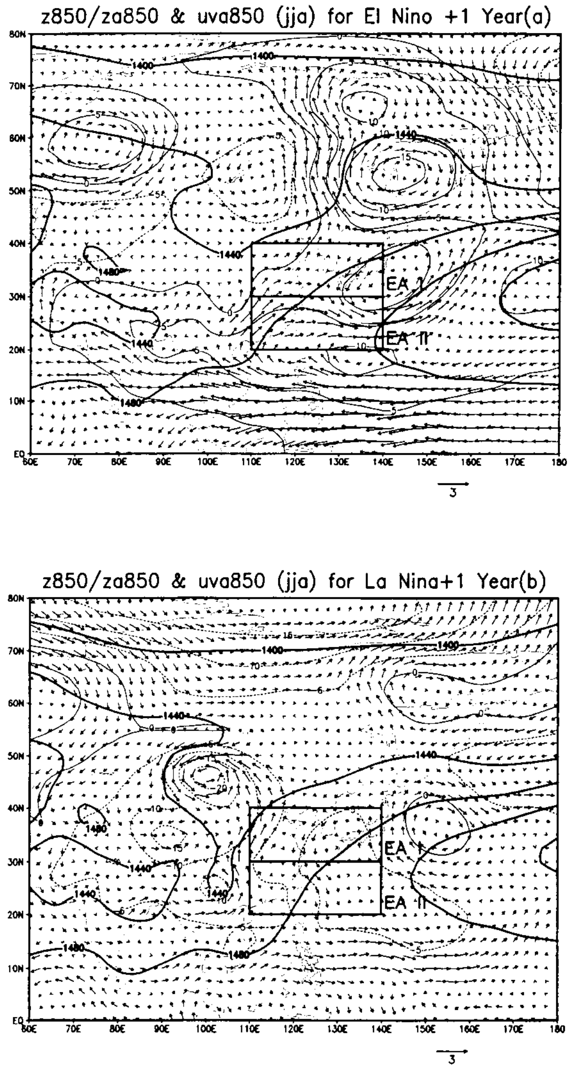

Fig. 10. Same as in Fig. 9 except for the 850 hPa winds anomaly (vector, ms^{-1}), geopotential height (thick line, contour interval: 40 gpm) and the height anomaly (thin line, contour interval: 5 gpm) in summer (a: decay El Niño years, b: decay La Nino years). Dashed lines show the negative anomalies.

tains respectively. The amplitude of anomaly of height is smaller here than that at 500 hPa. But the dipole around ~140°E indicates a blocking circulation in situ. On the other hand, the western end of the subtropical high (1520 contour line) extends much further westward and keeps a more southern location (20°N, 137.5°E) in Fig. 10a than it does (27°N, 147.5°E) in Fig. 10b, similar to the pattern EAMI composite in Figs. 2a and 2b. It could be also identified that the main body of the subtropical high is located to the southwest of the climatological position for a positive anomaly (over +10 gpm) is centered at 17.5°N, 132.5°E and a negative one (below zero gpm) at 30°N, 140°E respectively. This phenomenon could be seen more clearly than that at 500 hPa (refer to Figs. 9a and 9b). Wang et al. (2000) found that the anticyclonic circulation around the Philippine Islands tends to develop and maintain from mature to decay phase of El Niño episodes. Their finding may partly explain why the zonally westward expansion of the subtropical high in summer is associated with the preceding El Niño.

The circulation distributions from middle to low level troposphere in Figs. 9b and 10b are basically opposite from those in Figs. 9a and 10a, due to some position drift. Low values cover both the high and the low latitudes around East Asia in decaying La Nina years. The primary position of the subtropical high in decay La Nina years (Fig. 10b) is located to the northeast of that in decay El Niño years (Fig. 10a). However, Fig. 10b has somewhat different features from Fig. 2b. No strong northeasterlies in EA II area and southwesterlies in EA I area are found, in spite of the negative EAMI ($-0.97\ \mathrm{ms}^{-1}$).

The southern East Asian summer monsoon (i.e., in the EA II area) is basically quite strong (weak) associated with the preceding warm (cold) episode of ENSO. However, in the recent 23 years, La Nina conforming to the condition of SSTA3 below −0.7 ℃ in autumn occurs very infrequently. The Z500/Z850 anomaly in Figs. 9b and 10b does not well match up with the composite map of Fig. 2b. It is difficult to faithfully estimate the impact of La Nina on the East Asian summer monsoon. On the other hand, it is more meaningful to analyze the impact of mature phase of the warm episode in SON since the mature phases of El Niño tend to occur toward the end of the calendar year (Rasmusson and Carpenter 1982, Wang et al. 2000). Hereafter, we focus only on the impact of El Niño episodes.

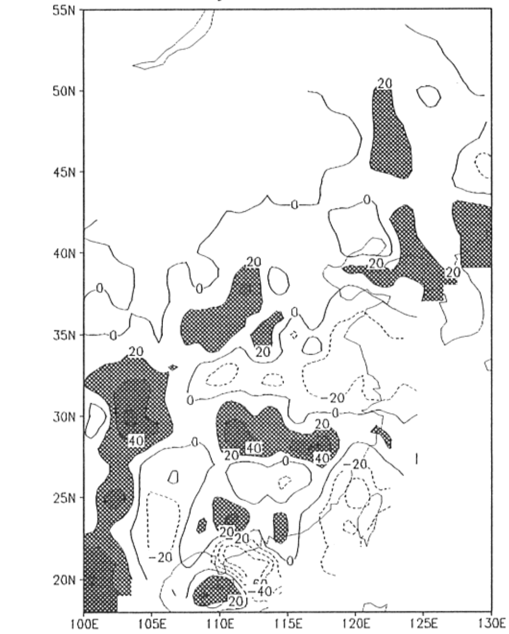

Fig. 11. Same as in Fig. 9 except for the rainfall in China (decay El Niño years, mm). Shaded areas show the value over 20 mm.

Figure 11 shows the composite maps of the rainfall anomaly around China in summer for the years when SSTA3 was over 1.5 ℃ during the preceding autumn. Positive rainfall anomalies are distributed in two belts. One rain belt spreads from 29°N, 103°E to east China, corresponding well to the positive correlation area in Fig. 3. The other one stretches from that point extending to the northeast district of China. The rain belts, especially the southern one, are distributed similarly to those in Fig. 1. Notice that the southern rain belt associated with the southwesterly wind anomaly at 850 hPa around EA II area agrees well as discussed in Section 3. The southern rain belt, located in between 27°N and 32°N, is a little on the southern side of the climatological position of the Meiyu belt (30~31°N). The northern rain belt is also associated with the positive southwesterly wind anomaly at 850 hPa around northeastern China, which is not the focal point in this study.

5. Typical case in 1997/1998

The unprecedented El Niño in '97/98 follows composite pictures. The Pacific warming reaches a peak in November of 1997. Then, the positive SST anomalies around the east central Pacific weakened

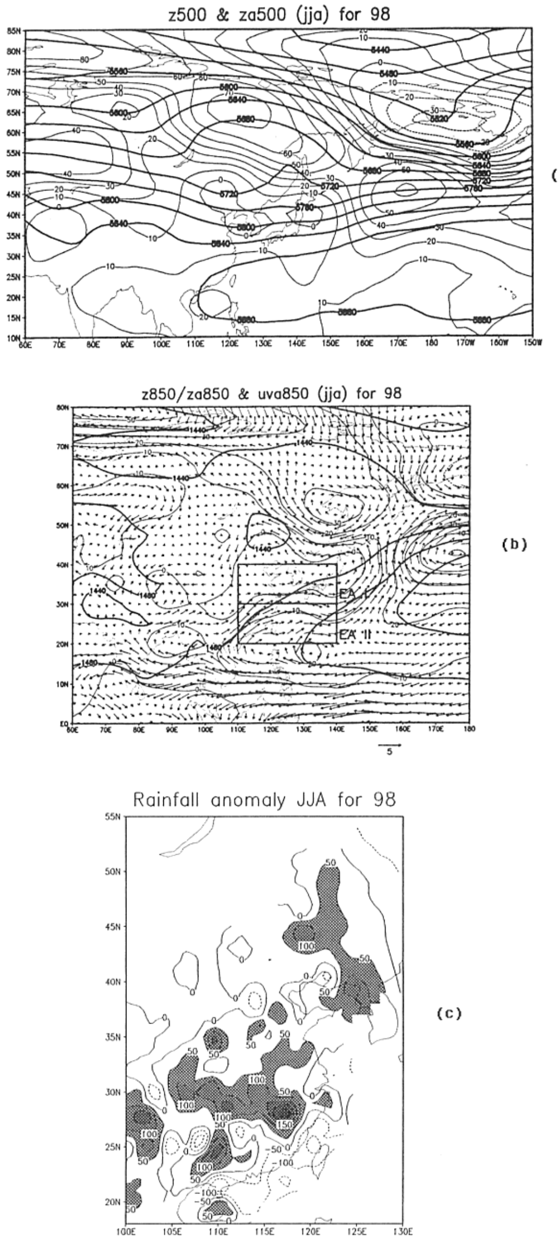

Fig. 12. 500 hPa geopotential height (thick lines, contour interval: 40 gpm) and its anomalies (thin lines, contour interval: 10 gpm) in summer of 1998 (a), 850 hPa winds anomaly (vector, ms^{-1}), geopotential height (thick line, contour interval 40 gpm) and the height anomaly (thin line, contour interval 10 gpm) in summer of 1998 (b) and rainfall anomaly (mm) in summer of 1998 (c). Dashed lines indicate negative anomalies and shaded areas show the value over 50 mm.

and finally, turned into negative anomalies in the summer of 1998. SSTA3 in SON and DJF reached 3.5℃ and 3.4℃ respectively, which is the strongest in the recent 50 years. The negative phase is maintained around northern Pacific during the whole period (figure omitted).

The spacial distribution in Figs. 12a and 12b is quite similar to that of the composite map of Figs. 9a and 10a. Large positive Z500 and Z850 anomalies associated with a huge blocking high are centered near the Okhotsk Sea in the summer of 1998 as shown in Figs. 12a and 12b. The subtropical high (5880 contour line) at 500 hPa extends westward to the Hainan Islands of China (18°N, 110°E); it extends further southward than normal. The position of the subtropical ridge in Fig. 12a extends 4–5 degrees of latitude further southward of that in Fig. 9a. Very strong southwesterly wind anomalies at 850 hPa prevail in the EA II area, but seldom in the EA I area. One strong positive rainfall anomaly area exists around northeastern China and the other much stronger anomaly belt is located in between 27°N and 30°N as shown in Fig. 12c. Note that the southern rainfall anomalies exceed 120 mm, a history record of heavy flood in situ (National Climate Center 1998). The patterns in Figs. 12c and 11 are basically similar except there is a weak positive rainfall anomaly around the Huaihe basin in Fig. 12c, whereas a negative anomaly exists in Fig. 11. All of the features in the '97/98 case well agree with the results summarized from El Niño composite analysis, but are more prominent.

6. Discussions and Summary

6.1 Discussions

The mechanism through which eastern Pacific warming can have a delayed impact on the East Asian monsoon from the following spring to early summer has been discussed recently by Wang et al. (2000). They noticed that a key system that bridges the eastern Pacific warming and the East Asian monsoon climate is the anticyclonic circulation anomalies located over the Philippine Sea. This anomalous anticyclone establishes prior to the warm peak in the Pacific and persists until the following summer due to in situ air-sea interaction, providing a delayed impact to the East Asian summer monsoon. The western Pacific Subtropical High anomalies found in this study are consistent with their results.

However, Wang et al. (2000) did not explore the delayed impacts of ENSO to the mid-high latitude circulation anomalies. The present study reveals that the high latitude blocking highs that favor Meiyu rainfall occur two or three seasons after the mature phase of the warm episode. Although the correlation maps (Figs. 6a and 6b) show a smaller significant positive area around the Cherski Mountains, the positive height anomaly is covered by quite a large area around higher latitudes of East Asia in the decay of El Niño episodes (see the composite Figures 9a and 10a). The positive anomaly center is rather close to the Okhotsk Sea in the composites. An important question needs to be addressed is: How does the East Asia blocking high (or strong ridge) form and persist during the decay of ENSO, affecting the East Asian summer monsoon? A possible explanation is as follows: In the case of the warm episode around the tropical eastern Pacific, the SSTA around high latitudes of the western North Pacific is negative which cools the atmosphere and lasts for two to three seasons (see Figs. 8a–d). On the other hand, the continent between Siberia and the Okhotsk Sea is heated rapidly by strong solar radiation in the boreal summer, which could warm up adjacent continent air. Thus, a strong temperature gradient would be established in the middle troposphere between the continent and the Northwest Pacific oceans in summer. The persistent anticyclone in the area, 50–70°N, 131–150°E and the Aleutian low are possibly intensified by the land-ocean thermal contrast, so that the blocking anticyclones around East Asia become active (Wang 1993). Okawa (1973 and 1976) suggested that the land-sea thermal contrast between the Siberia and Bering Seas plays an important role in developing the Okhotsk high, whose point of view supports our suggestion. This mysterious mechanism needs to be analyzed further.

We analyzed EAMI from 1958 to 1998. It is identified that (1) almost all of the features of the EAMI in 41 years' period are the same as those in 23 years' period (1976–1998), and (2) however, the correlation between EAMI and WYI in 41 years' period is poorer than that in 23 years' period. Kawamura et al. (1998) pointed out that the Asian monsoon-ENSO interaction may be more active in recent years (1979 to 1993) than before (1963 to 1977). In fact, the correlation pattern in Figs. 6a and 6b is more prominent by using 23 years' data. The positive correlation center around the Cherski Mountains drifts southwards about two latitude degrees and reaches 98% confidence level in recent 23 years. Meanwhile, the significant positive correlation area covered with low latitudes is stronger to the west of the Philippine Islands (figure omitted). These results are consistent with Kawamura et al. (1998). Considering the distinct climate difference from decadal to vicennial scale, we only focus on recent interannual variability of EAMI. Recent EAMI can also give more information of its latest tendency of the variability, which could more clearly show not only a recent relationship between the East Asian summer monsoon and South Asian summer monsoon but also their different impact by ENSO. The significant negative correlation between the two indices also indicates that the East Asian summer monsoon and the broad-scale Asian summer monsoon are not independent systems, especially in the recent 23 years, although they exhibit different behavior. The relationship between the distribution pattern of the East Asian summer monsoon and the strength of the broad-scale Asian summer monsoon deserves further study.

Zhang et al. (1996) pointed out that the mature phase of El Niño is associated with the strong East Asian summer monsoon simultaneously. However, the relationship is based on a limited data sample. The significant negative correlation area around 42.5°N, 150°E in Figs. 6c and 6d implies that low height around the negative region tends to occur almost simultaneously when El Niño develops in summer. But as discussed above, the East Asian summer monsoon is more related with the evolution of the height field around the western Pacific (equatorward of 30°N), as related to the subtropical high. At the same time, there is a less dramatic significant area of positive correlation centered at 25°N, 147.5°E; this area is too far from the EA I and EA II areas and has less influence compared with that of Figs. 6a and 6b. Summer EAMI is poorly correlated ($r = 0.227$), with the concurrent SST3 and most mature El Niño events occur in the end of a calendar year as mentioned above. This tendency lays the stress on the delayed impact of El Niño on the East Asia summer monsoon due to the significant correlation ($r = 0.487$) between summer EAMI and the preceding autumn SST3[2].

6.2 Conclusions

The present study has investigated the lagged relation of ENSO event with the East Asian sum-

2 Refer to the time series of EAMI in Fig. 5 and the SSTA3 in SON in Fig. 7. The time series of SSTA3 in JJA is omitted.

mer monsoon by using correlation and composite analysis. The composite results are confirmed by the '97/98 case analysis. The following results were obtained:

(1) A new index called EAMI for measuring the East Asian monsoon was defined, which could extensively describe the south-north distribution of the East Asian summer monsoon's activity. The interannual variability of the EAMI displays a significant negative correlation with the broad-scale Asian monsoon index proposed by Webster and Yang (1992) from 1976 to 1998.

(2) A significant positive correlation between the summer 500 hPa geopotential height anomalies and the NINO-3 SST in the preceding fall and winter is found in the subtropical East Asia/western North Pacific, and in the northeast Asia centered at 70°N, 137.5°E. A strong (weak) summer monsoon in subtropical East Asia tends to occur about two to three seasons after the NINO-3 SST anomalies exceed 1.5 ℃ (drop below −0.7 ℃).

(3) The above results indicate a delayed impact of the ENSO on the East Asian summer atmosphere circulation. During the summer after the El Niño reaches its mature phase, an anomalous blocking anticyclone tends to occur in northeast Asia, meanwhile the western North Pacific subtropical high extends abnormally westward. This anomalous circulation pattern enhances the summer monsoon in subtropical East Asia. The above mentioned evolution of the circulation anomalies becomes more prominent in the unprecedented '97/98 El Niño event, suggesting that the devastating 1998 flood in south central China may be partially due to the delayed impact of the '97/98 El Niño.

Acknowledgments

We thank Ms Hee-Jeong, Back, Miss Jung-Hee Ryu and Mr. Seung-Won Yi, METRI, Korea, and Dr. Maj Roohr in the U.S. Air Force of Korea, and R. Wu of the University of Hawaii, USA for their assistance. Special thanks are extended to Dr. Jun Matsumoto, Tokyo University. This research was performed under Natural Hazards Prevention Research Project, one of the Critical Technology-21 Programs, funded by the Ministry of Science and Technology of Korea, and supported by NSFC No. 49794030 and MSTC (G1998040908).

References

Bjerknes, J., 1966: A possible response of the atmospheric Hadley circulation to equatorial anomalies of ocean temperature. *Tellus*, **18**, 820–829.

———, 1969: Atmospheric teleconnections from the equatorial Pacific. *Mon. Wea. Rev.*, **97**, 163–172.

Chen, L. And M. Dong, and Y. Shao, 1992: The characteristics of interannual variation on the East Asian monsoon. *J. Meteor. Soc. Japan*, **70**, 397–421.

Ding, Y., 1994: Monsoons over China. Kluwer Academic Publishers, 419pp.

Kalnay, E., and Coauthors, 1996: The NCEP/NCAR 40year reanalysis project. *Bull. Amer. Meteor. Soc.*, **77**, 437–471.

Kawamura, R., 1998: A possible mechanism of the Asian summer monsoon-ENSO coupling. *J. Meteor. Soc. Japan*, **76**, 1009–1027.

———, M. Sugi, T. Kayahara, and N. Sato, 1998: Recent extraordinary cool and hot summers in East Asia simulated by an ensemble climate experiment. *J. Meteor. Soc. Japan*, **76**, 597–617.

Lau, K.M., K.M. Kim, and S. Yang, 2000: Dynamical and boundary forcing characteristics of regional components of the Asian summer monsoon. *J. Climate*, **13**, 2461–2482.

Mooley, D. and B. Parthasarathy, 1983: Variability of the Indian summer monsoon and tropical circulation features. *Mon. Wea. Rev.*, **111**, 967–978.

National Climate Center, China, 1998: *Super flooding and climate abnormality in China in 1998.* Meteorological Press China, 139pp (in Chinese).

Ninomiya, K. and C. Kobayashi, 1998: Precipitation and moisture balance of the Asian summer monsoon in 1991. Part I: Precipitation and major circulation systems. *J. Meteor. Soc. Japan*, **76**, 855–877.

——— and ———, 1999: Precipitation and moisture balance of the Asian summer monsoon in 1991. Part II: Moisture transport and moisture balance. *J. Meteor. Soc. Japan*, **77**, 77–99.

Okawa, T., 1973: Growth mechanism of the Okhotsk high. *J. Meteor. Res.*, **25**, 65–77 (in Japanese).

———, 1976: Behavior of Okhotsk High and 500-mb level flow pattern in the Bai-u season. *J. Meteor. Res.*, **28**, 253–261 (in Japanese).

Rasmusson, E.M., and T.H. Carpenter, 1982: Variations in tropical sea surface temperature and surface wind fields associated with the Southern Oscillation/ El Niño. *Mon. Wea. Rev.*, **110**, 354–384.

Reynolds, R.W. and T.M. Smith, 1994: Improved global sea surface temperature analyses using optimum interpolation. *J. Climate*, **7**, 929–948.

Tao, S. and L. Chen, 1987: A review of recent research on the East Asian summer monsoon in China. In *Monsoon Meteorology*, Eds. C-P. Chang and T.N. Krishnamurti, 60–92.

Walker, G.T. and E.W., Bliss, 1932: World weather. *V. Mem. R. Meteorol. Soc.*, **4**, 53–84.

Wang, B. and Z. Fan, 1999: Choice of South Asian summer monsoon indices. *Bull Amer. Meteor. Soc.*, **80**, 629–638.

———, R. Wu and Xiouhua Fu, 2000: Pacific-the East Asian teleconnection: How does ENSO affect the East Asian climate? *J. Climate*, **13**, 1517–1536.

Wang, Y., 1992: Effects of blocking anticyclones in Eurasia in the rainy season (Meiyu/Baiu season). *J. Meteor. Soc. Japan*, **70**, 929–951.

———, 1993: *Role of persistent anticyclones in Eurasia in the rainy season (Meiyu/Baiu season)*. Ph. D. dissertation, Iinstitute of Geoscience, Univ. Tsukuba, 130pp.

——— and Y. Song 1998: A diagnostic analysis on the growth mechanism of the East Asia blocking high in 1991. *Acta Meteor. Sinic, China*, **56**, 212–223 (in Chinese with English abstract).

Webster, J.P. and S. Yang, 1992: Monsoon and ENSO: Selectively interactive systems. *Quart. J. Roy. Meteor. Soc.*, **118**, 877–926.

Wyrtki, K., 1975: El Niño: The dynamic response of the equatorial Pacific Ocean to atmospheric forcing. *J. P hys. Oceanogr.*, **5**, 572–584.

Yang, S., and K.-M. Lau, 1998: Influences of sea surface temperature and ground wetness on Asian summer monsoon. *J. Climate*, **11**, 3230–3246.

Ye, D., R. Huang, 1996: *Study about mechanism of drought and flood around Changjiang river and Huanghe river*. Shandong Science and technique press, 387pp (in Chinese).

Zhang, R., A. Sumi and M. Kimoto, 1996: Impact of El Niño on the East Asian Monsoon: A diagnostic study of the '86/87 and '91/92 events. *J. Meteor. Soc. Japan*, **74**, 49–62.